Journal of Applied Polymer Science

Thermophysical properties of bacterial poly(3-hydroxybutyrate): Characterized by TMA, DSC, and TMDSC

Liqing Wei, Armando G. McDonald
Renewable Materials Program, Department of Forest, Rangeland and Fire Sciences, University of Idaho, Moscow, Idaho 83844-1132
Correspondence to: A. G. McDonald (E-mail: armandm@uidaho.edu)

ABSTRACT: The melting, isothermal and nonisothermal crystallization behaviors of poly(3-hydroxybutyrate) (PHB) have been studied by means of temperature modulated differential scanning calorimetry (TMDSC) and conventional DSC. Various experimental conditions including isothermal/annealing temperatures (80, 90, 100, 105, 110, 120, 130, and 140°C), cooling rates (2, 5, 10, 20, and 50°C/min) and heating rates (5, 10, 20, 30, 40, and 50°C/min) have been investigated. The lower endothermic peak (T_{m1}) representing the original crystals prior to DSC scan, while the higher one (T_{m2}) is attributed to the melting of the crystals formed by recrystallization. Thermomechanical analysis (TMA) was used to evaluate the original melting temperature (T_{melt}) and glass transition temperature (T_g) as comparison to DSC analysis. The multiple melting phenomenon was ascribed to the melting-recrystallization-remelting mechanism of the crystallites with lower thermal stability showing at T_{m1}. Different models (Avrami, Jeziorny-modified-Avrami, Liu and Mo, and Ozawa model) were utilized to describe the crystallization kinetics. It was found that Liu and Mo's analysis and Jeziorny-modified-Avrami model were successful to explain the nonisothermal crystallization kinetic of PHB. The activation energies were estimated in both isothermal and nonisothermal crystallization process, which were 102 and 116 kJ/mol in respective condition. © 2015 Wiley Periodicals, Inc. J. Appl. Polym. Sci. **2015**, *132*, 42412.

KEYWORDS: biopolymers and renewable polymers; crystallization; differential scanning calorimetry

Received 13 February 2015; accepted 23 April 2015
DOI: 10.1002/app.42412

INTRODUCTION

Polyhydroxyalkanoates (PHAs) is a family of renewable bioplastics which are produced by microbial biosynthesis and stored by bacteria as energy reserves.[1] Poly(3-hydroxybutyrate) (PHB), the predominate biopolymer of PHAs, has been studied most extensively and considered as rigid material with thermal properties close to polypropylene.[2,3] Its biodegradation but low permeability for water vapor have great potential in food packaging industry.[4] However, its high degree of crystallinity (~60%) resulting in the formation of large crystal spherulites and the mechanical properties are poor if the size of these spherulites exceed a critical level, and therefore PHB is always considered as brittle thermoplastic.[3,5,6] Therefore, improving the thermomechanical properties of PHB and/or its blends with other natural/synthetic polymers is a popular subject, especially in the field of crystallization studies in relation to its semicrystalline structure.[7–10]

The crystallization behavior of a polymer tells whether the polymer crystals can be present under certain external conditions, while its speed to finish crystallization is determined by the kinetics of the crystallization process.[11] To summarize the studies of crystallization of different polymers in the past, there are two main conditions: (i) the isothermal crystallization, keeping the external environments (i.e., cooling/heating rates and thermal gradients) constant and (ii) the nonisothermal crystallization as a compensation to (i), considering the changes of external conditions which can reflect industrial processing situation.[11] Most studies on PHB just focused on a relatively narrow range of isothermal temperatures that is close to or just slightly above its cold crystallization onset temperature (T_c) in case (i).[12] However, in the processing of PHB (or its copolymer) products from melt, such as injection molding and extrusion, the temperature of the mold is set far lower or higher than the T_c.[13] In other words, isothermal crystallization of the injection molded PHB products always occurred at temperatures much lower or higher than its T_c. Therefore, to understand the kinetics of isothermal crystallization in a wider temperature range is necessary to give guidance to process PHB effectively. In either (i) or (ii) of conditions of different classes of polymers including PHB, various theories/models have been proposed, modified and reviewed.[11,14] Generally, in these studies the

samples are quenched below their glass transition temperature (T_g) from melt then heated to melt the sample again, which is namely known as cold crystallization process. Nevertheless, in the industrial scale polymers are usually processed in the molten state and the properties of polymer are determined by the resulting crystalline structure of the product from melt, while the melting behavior is influenced by the crystallization process history.[5,15] To explain the phenomena models are developed such as the classic Avrami model to evaluate the kinetics of isothermal crystallization; while the Ozawa analysis model is widely used for nonisothermal crystallization of polymers but always failed because it neglects secondary crystallization.[12] Other models have been developed to improve model predictability. For example, Liu and Mo's model was found to be successful to explain the nonisothermal crystallization of the bioplastic, poly(lactic acid) (PLA)/PHB blends,[5] while Jeziorny-modified-Avrami model was applicable to poly(butylene terephthalate) (PBT) and its composite.[15] Hence, nonisothermal crystallization behavior of semicrystalline PHB is also expected to be explained by these models.

Meantime, the subsequent melting behavior after crystallization can attract more attention in the fields of both academia and industry. Double or multiple melting endothermic behaviors are usually found in semicrystalline polymers melts by differential scanning calorimetry (DSC), which are crystallized isothermally at selective crystallization temperatures or nonisothermal conditions at various cooling rates.[16] However, the documented data on multiple or double melting behavior of PHB following the isothermal or nonisothermal crystallization processes is limited. Temperature modulated DSC (TMDSC) experiments can obtain more accurate heat capacity measurements and separate thermodynamic phenomena (e.g., glass transition, crystallization and melting behavior) with better resolution and sensitivity.[18] This technique was used to examine the crystallization and multiple melting behavior of PHB by Guanratne *et al.*[17] In their study, the effects of isothermal crystallization and crystallization rates on the multiple melting behavior of PHB were determined, but conducted in a relatively small temperature range (100–120°C) and the kinetics were not addressed. Whereas many industrial processes, such as injection molding and extrusion, involve isothermal crystallization in the mold or die in which the temperature was generally set beyond the range studied for PHB.[18] Isothermal/nonisothermal crystallization processes were also shown to play a crucial role in the melting behavior of other semicrystalline polymers, such as poly(butylene succinate) (PBSU) and poly(ethylene succinate) (PES),[16] poly(ethylene terephthalate) (PET) and poly(ethylene 2,6-naphthalene dicarboxylate) (PEN),[19] and isotactic polystyrene (iPS).[20] Various reasons have been attributed to the multiple melting behavior of semicrystalline polymers, such as the melting, recrystallization, and remelting (MRR) during DSC heating scans, resulting in the presence of crystal modifications and different molecular species present in the polymer systems.[21] However, controversies still exist as to the exact origins of the multiple melting behavior of PHB.

The aim of this study was to investigate the influence of isothermal annealing of PHB (over a wide temperature range) on the nonisothermal cold crystallization process from melt at different cooling rates by DSC and TMDSC. Meanwhile, the cold crystallization behavior and the kinetics were studied using different models including the Liu and Mo's and Jeziorny-modified-Avrami models to evaluate the nonisothermal crystallization kinetics of PHB for the first time. The developed models will give insight as to the mechanism of the crystallization process for PHB and its multiple melting behavior, especially the nonisothermal crystallization induced multiple melting phenomenon. Thermal mechanical analysis (TMA) was employed to identify the original (or true) melting temperature (T_{melt}) as a comparison to the DSC and TMDSC melting transitions.

EXPERIMENTAL

Materials and Sample Preparation

The commercial grade PHB was obtained from Tianan Biopolymer Inc. (Ningbo, China). The PHB was purified to remove any additives in the commercial preparation before analysis. PHB powder was dissolved in chloroform, precipitated in cold petroleum ether (boiling point range 35–60°C), recovered by filtration and dried under vacuum for at least one week prior to use in order to remove any excess moisture/solvent. The weight average molar mass (M_w) = 290 kg/mol and polydispersity (PD) = 2.3 was determined by size exclusion chromatography (SEC).[22]

Thermomechanical Analysis

The thermomechanical properties were characterized using Perkin Elmer TMA7 instrument equipped with a penetration probe (0.01 N applied load). PHB sample was molded into a rectangular bar using a Dynisco Lab Mixer Extruder. For the thermomechanical analysis (TMA) analysis a small piece (in triplicate, 2 × 1 × 1 mm^3) was cut from the molded bar and heated from −50 to 190°C at a rate of 5°C/min. The T_g and T_{melt} were determined from the onset point of softening.

Differential Scanning Calorimetry and Temperature Modulated DSC

Conventional DSC and TMDSC were performed on PHB (4–6 mg, in triplicate) using a TA Instruments model Q200 DSC with refrigerated cooling. All the samples were heated rapidly at 100°C/min to 180°C to remove any thermal history.

For the isothermal crystallization kinetics study, samples were held isothermally at 180°C for 5 min to allow for complete melting to occur, followed by rapid cooling (50°C/min) to the target isothermal crystallization temperature (T_{iso} = 80, 90, 100, 105, 110, 115, 120, 130, and 140°C). All samples were held at T_{iso} for 1 h after which PHB crystallization was believed to be complete. The relative degree of crystallinity, $X_{t\text{-}iso}$, after time t, was determined according to the equation:

$$X_{t-iso} = \int_0^t (dH/dt)dt \Big/ \int_0^\infty (dH/dt)dt \quad (1)$$

where the first integral is the heat released after time t and the second integral is the total heat of the whole crystallization process, for $t = \infty$; the activation energy of crystallization, E_{iso}, was calculated as follows:

$$V_c = A \exp(-E_{iso}/RT_{iso}) \quad (2)$$

where V_c is the crystallization rate determined from the slop of the linear region of $X_{t\text{-}iso}$ vs. t plot, A is an arbitrary pre-exponential factor, R is the gas constant.

In order to investigate the effect of isothermal annealing on the subsequent melting behavior of PHB, a wider range of isothermal annealing temperature (T_a = 80, 90, 100, 105, 110, 120, 130 and 140°C) was selected. In this study, PHB melts were rapidly cooled to T_a at −50°C/min and held for 1 h followed by the heating TMDSC measurements to 200°C, at an average heating rate of 2°C/min with a period of 60 s and modulation amplitudes of ±0.6°C. The control (unannealed) sample was treated with a similar procedure in that the polymer melt was cooled to −50°C and then heated to 200°C directly without being annealed.

The nonisothermal crystallization test of PHB melts was performed at various cooling rates (ϕ) of 2, 5, 10, 20, and 50°C/min, respectively, to −50°C. The T_c, crystallization peak temperature (T_p) and the temperature at which crystallization was complete (T_e) were determined from the cooling scan. The effects of nonisothermal crystallization on the melting behavior of PHB were investigated by reheating the samples from −50 to 200°C at a heating rate of 10°C/min by either the conventional DSC or TMDSC measurements with an average heating rate of 2°C/min with a period of 60 s and modulation amplitudes of ±0.6°C. From the heating scan the T_g was determined.

The effect of heating rate (Φ) on the multiple melting behaviors was investigated after polymer melts were cooled down to −50°C rapidly at a cooling rate of 80°C/min and held for 5 min, and then heated to 200°C at Φ = 5, 10, 20, 30, 40, and 50°C/min. Both conventional DSC and TMDSC data were analyzed using TA Universal Analysis v4.4A software.

RESULTS AND DISCUSSION

Melting Temperature Obtained by TMA

TMA penetration provides excellent means of assessing T_g and T_{melt} of material in the compression mode by recording the displacement (%) as function of temperature. Below the T_{melt} of PHB the sample undergoes a slight expansion, while the temperature was above the T_g the sample softens and if the temperature was above T_{melt} the sample melts and the lightly loaded probe penetrates the sample and a rapid decrease in the thickness of the sample was observed. The T_g and T_{melt} of the PHB were determined to be about 5 ± 1°C and 167 ± 0.5°C, respectively (Figure 1). These values were in close agreement with the literature.[6,23]

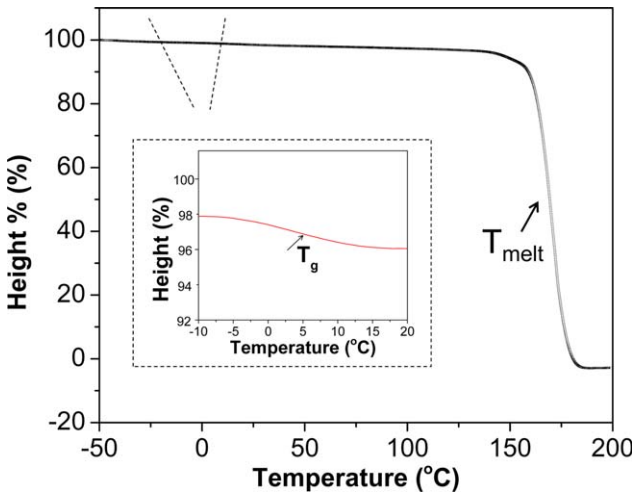

Figure 1. TMA thermograms of PHB samples. Note: arrows pointed to T_g and T_{melt}. [Color figure can be viewed in the online issue, which is available at wileyonlinelibrary.com.]

Isothermal Crystallization Behavior and Kinetics

One property of a polymer that will have an impact on processing or end use of the final product is the crystallization behavior of the polymer. The primary method used to understand the crystallization of polymer is isothermal crystallization, especially the kinetics involved. Therefore, in this section, the isothermal crystallization kinetics of PHB was studied at selected temperatures (T_{iso}). A conventional DSC was used by following the classical scans that the polymer was first heated to the molten state and then quench-cooled rapidly to the desired T_{iso} and held for sufficient time (1 h) for the crystallization process to be complete and the heat flow signal reaches the baseline. Figure 2(a) shows the relative crystallization evolution ($X_{t\text{-}iso}$ vs. time t) of PHB. The crystallization rate (V_c), crystallization half time ($t_{cry-1/2}$) and activation energy (E_{iso}) were determined and summarized in Table I. When the T_{iso} was increased from 80 to 140°C, the crystallization rate was reduced significantly, hence the $t_{cry-1/2}$ was increased and a longer overall time was required to complete the crystallization process. The activation energy (E_{iso}) of the isothermally crystallized PHB in this study was 102 kJ/mol. Previous kinetic studies of commercial PHB (Sigma-Aldrich, US) on the isothermal crystallization at a narrower temperature range (100–120°C) showed a lower activation energy of 87.3 kJ/mol with M_w = 230 kg/mol and PD = 2.6.[24] The higher M_w (290 kg/mol) in this study suggests longer polymer chains present in the polymer system and the more tangled up they will get, and hence a lot more energy will be required to diffuse these long chains into the crystalline lattice during crystallization process.[8]

The isothermal crystallization kinetics of PHB and its copolymer (polyhydroxybutyrate-co-hydroxyvalerate, PHBV) in a relatively narrower temperature range have been explained successfully by Avrami equations:[22,25]

$$1 - X_{t\text{-}iso} = \exp(-kt^n) \quad (3)$$

Equation (3) can be written in double-logarithmic form as:

$$\ln[-\ln(1 - X_{t-iso})] = \ln k + n \ln t \quad (4)$$

where k and n are the Avrami rate constant and Avrami exponent at time t, respectively, which depend on both the nucleation mechanism and the growth geometry.[22,26]

The Avrami plot ($\ln[-\ln(1 - X_{t\text{-}iso})]$ vs. $\ln t$) of the data from Figure 2(a) and Table I is shown in Figure 2(b). The experimental data fitted very well with the Avrami equation at different T_{iso} = 80, 90, 100, 105, and 110°C. However, when the T_{iso} was increased to ≥ 115°C the initial linear relationship was observed

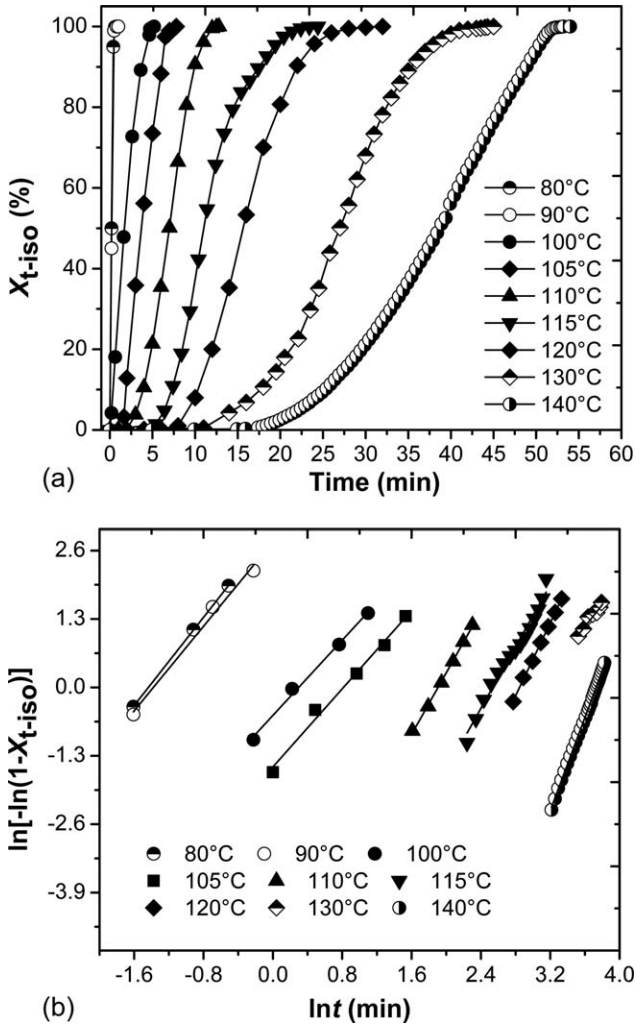

Figure 2. (a) Plot of relative crystallinity, $X_{t\text{-iso}}$ (%), as function of time, t, and (b) Avrami plot of $\ln[-\ln(1 - X_{t\text{-iso}})]$ versus $\ln t$ at different isothermal temperatures ($T_{iso} = 80$, 90, 100, 105, 110, 115, 120, 130, and 140°C) as determined by conventional DSC.

followed by a slight leveling off. This phenomenon could be contributed to the secondary crystallization of PHB due to slow crystallization of the crystal defects, or the spherulite impingement in the later stage of the whole crystallization process at higher T_{iso}. From the slope and intercept of each fitted line from Figure 2(b), the Avrami parameters, the Avrami exponent (n) and overall crystallization rate constant (k), were determined respectively. In addition, the half time, $t_{Avrami\text{-}1/2}$, to complete the crystallization process was obtained by the equation:[5,13]

$$t_{Avrami\text{-}1/2} = (\ln 2/k)^{1/n} \quad (5)$$

and the overall rate of crystallization was evaluated by $k^{1/n}$. These values are summarized in Table I. The $k^{1/n}$ values decreased with increasing T_{iso}, suggesting the whole crystallization process can be finished in a shorter time period, which was supported by lower $t_{Avrami\text{-}1/2}$ and $t_{cry\text{-}1/2}$ values at lower T_{iso}. The calculated $t_{Avrami\text{-}1/2}$ values were close to the data from $t_{cry\text{-}1/2}$. For example, the $t_{cry\text{-}1/2}$ at $T_{iso} = 80$ and 90°C was only seconds, while 40 min was required to reach 50% crystallization at $T_{iso} = 140$°C. These values were slightly higher than other studies, which may be attributable to its higher M_w in this study resulting in the relative lower crystallization rates. At different T_{iso}'s the n values varied between 1.8 to 4.8, which could be attributed to the heterogeneous nucleation mechanism and geometry of PHB crystal growth.[22,26] These studies indicated the isothermal crystallization temperatures in accompanied with the crystallization kinetics strongly influence the end-use thermomechanical properties (tensile strength, elongation to break, and transition temperatures) of pure PHB. It is therefore concluded that the isothermal crystallization temperatures could greatly determine practical applications of PHB.

Influence of Isothermal Annealing Temperatures to Melting Behavior of PHB

Isothermal annealing temperatures have a significant impact on the melting behavior of PHB. Figure 3 shows the melting curves of total and reversing heat flow curves by TMDSC for samples annealed at different temperatures. The annealing time was 1 h. The results show clearly that the melting behavior was different for different annealing temperatures at the same fixed annealing time and identical cooling/heating rate. The melting enthalpy was higher after annealing as compared with the control sample. From Figure 3, three endothermic peaks were observed after annealing (labeled as T_{ap}, T_{m1}, and T_{m2} in the order of

Table I. The Crystallization Rate (V_c, Determined from $\ln V_c$ vs. $1/T_{iso}$), Crystallization Half Time ($t_{cry\text{-}1/2}$, Determined from $X_{t\text{-iso}}$ vs. t plot), Isothermal Activation Energy (E_{iso}), Crystallization Half Time ($t_{Avrami\text{-}1/2}$, Calculated from Avrami Parameters, n and k), and the Overall Rate of Crystallization, $k^{1/n}$

T_{iso} (°C)	V_c (min^{-1})	$t_{cry\text{-}1/2}$ (min)	E_{iso} (kJ/mol)	$t_{Avrami\text{-}1/2}$ (min)	n	$k^{1/n} \times 10^{-4}$ (min^{-1})
80	3.8	<1.0		0.1	2.09	42,177
90	3.3	<1.0		0.2	2.01	39,634
100	0.38	1.2		1.1	1.82	7479
105	0.34	3.6	102	2.2	1.83	3678
110	0.16	6.1		3.7	2.01	2252
115	0.13	10.1		8.7	2.00	956
120	0.10	15.4		14.4	2.08	583
130	0.05	27.2		28.8	2.22	294
140	0.04	38.8		38.6	4.80	240

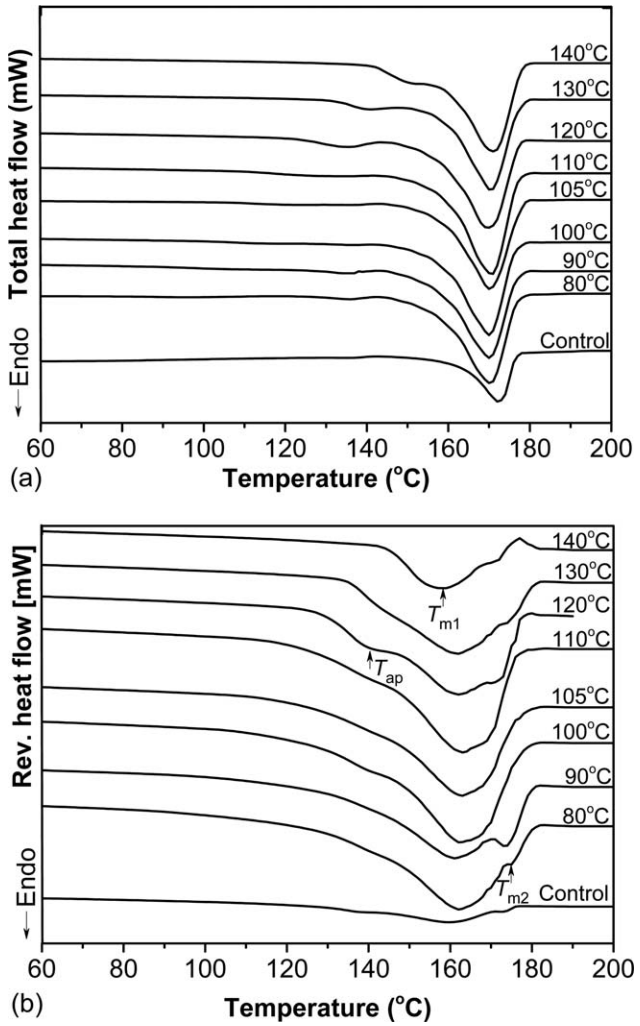

Figure 3. (a) TMDSC total heat flow curves and (b) reversing (Rev.) heat flow curves of control sample and samples isothermally annealed at different temperatures. The curves are shifted vertically for clarity.

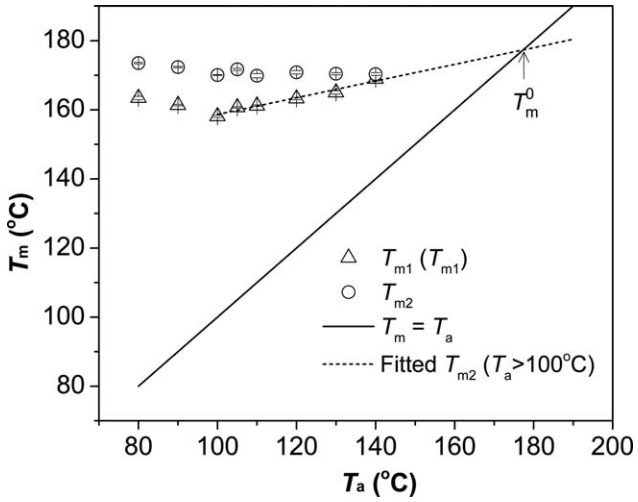

Figure 4. Plot of melting temperatures (T_{m1} and T_{m2}) versus different T_a's for PHB. The transition temperatures were determined and averaged from triplicate TMDSC reversing heat flow curves as shown in Figure 3b with standard deviation showed as error bars. Extrapolation of T_m^0 from the melting temperature as a function of T_a's of PHB.

temperature from low to high). T_{m1} and T_{m2} were easier to be identified in the reversing heat flow curve [Figure 3(b)] than in the total heat flow curve [Figure 3(a)]. The annealing peak (T_{ap}) shifted to higher temperature with increasing T_a and the T_{ap} was always at about 15–20°C above T_a. The similar phenomenon was observed for isothermally crystallized PET.[27,28] They concluded that the annealing peak was associated with the fusion of defective secondary lamellae, which melt earlier because of their lower stability.

The variations of the melting transition (T_{m1} and T_{m2}) with T_a are shown in Figure 4. T_{m1} decreased to a minimum value when T_a <100°C; when T_a >100°C, with increasing T_a, the T_{m1} shifts to higher temperatures and finally merges into the highest endotherm (T_{m2}). With an increase of T_a, T_{m2} remains constant at ca. 170°C. T_{m1} was attributed to the melting of original crystals formed before the DSC scan, and the T_{m2} was associated with the melting of the recrystallized components during heating scan.[29] The origin of double melting was probably due to the MRR mechanism during the TMDSC reheating scan,[23] whereas the initial decrease of T_{m1} could be attributed to the thicker crystal lamella formed at lower T_a (<100°C) in this study. These results are in agreement with the isothermally induced multiple melting behavior of PET.[27] When measuring the crystallinity of a polymer, TMDSC observes the formation of crystalline structures as soon as the sample starts to melt, and this phenomenon is known as recrystallization and might not be detected by conventional DSC.[30,31] The recrystallization process is evaluated by the degree of undercooling, $\Delta T = T_m^0 - T_m$, where the T_m^0 is the ideal equilibrium melting temperature of PHB. According to the method of Hoffman and Weeks,[32] the T_m^0 was obtained by plotting the T_m versus T_a, extrapolation of experimental data (used T_{m2} for T_a >100°C) to the intersection of $T_m = T_a$ yields T_m^0 which was estimated to be 177.3°C (Figure 4). T_m was the experimental melting temperature (T_{m1} was used). The ΔT is interpreted as the driving force of recrystallization in semicrystalline polymers.[21,33] At higher T_a, T_{m1} was shown to increase, resulting in a decrease of ΔT so that less driving force was available to move PHB toward recrystallization. Hence, the double melting peaks started to merge gradually when T_a increased from 100 to 140°C; while two melting endotherms were clearly observed for T_a <100°C. In other words, at higher T_a, the rate at which the equilibrium state is reached will be faster. Therefore, higher isothermal annealing temperature will inhibit the recrystallization behavior.

Montserrat and coworkers showed that the total heat flow was a suitable parameter to be used to calculate the crystallinity for PET by TMDSC.[19] Hence, the degree of crystallinity (χ_c %) for PHB in the isothermal crystallization study was calculated using the equation:[4,34]

$$\chi_c\% = \Delta H_m / \Delta H_0 \times 100 \quad (6)$$

where ΔH_m is the melting enthalpy obtained from the total heat flow curve [Figure 3(a)] and ΔH_0 is melting enthalpy of 100% crystalline PHB (146 J/g).[4] The results of χ_c% versus different T_a's, as given in Figure 5, indicate (i) when the T_a is <100°C

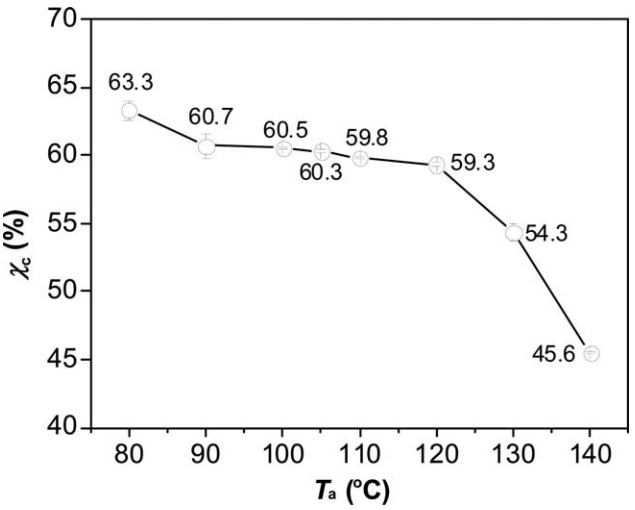

Figure 5. Plot of PHB crystallinity, χ_c (%), vs. annealing temperature, T_a, and the averaged values from triplicates are labeled with standard deviation was shown as error bars.

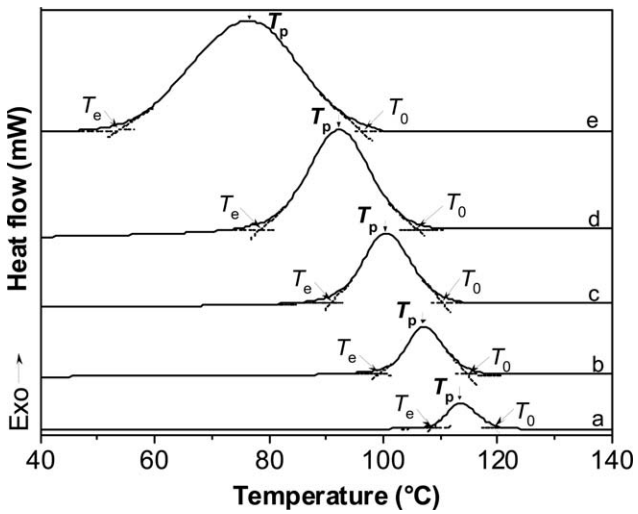

Figure 6. DSC curves showing exothermic curves in nonisothermal crystallization process at various cooling rates (a: 2; b: 5; c: 10; d: 20, and e: 50°C/min). The curves are shifted vertically for clarity.

the degree of crystallinity (χ_c %) of PHB decreases from 63.3% to 60.5% with an increase of T_a from 80 to 100°C; (ii) when 100°C < T_a > 120°C, the crystallinity seems to be around 60%; if (iii) the T_a is >120°C the degree of crystallinity decreases significantly from 59.3 to 45.6% with increasing the respective annealing temperature from 120 to 140°C. This shows that at higher T_a, a greater driving force was required to align polymer chains and crystallize accordingly. This result would provide a profound insight into the relationship between thermal history during processing and the property of end product (especially the crystallinity and mechanical properties). In other words, in the manufacturing of PHB products such as injection molding, different mold temperatures can be selected to tailor the crystallinity of the final products, which will affect their corresponding thermophysical properties accordingly. This further confirmed that PHB product properties depending on the crystallinity and crystallization history of polymers, can be affected by annealing conditions after PHB samples are prepared and prior to be tested.

Influence of Nonisothermal Crystallization

Figure 6 shows nonisothermal crystallization exothermic DSC curves versus temperature at various ϕ for PHB from the melt. It was seen that increasing ϕ resulted in a smaller exothermic peak. This resulted in less time being available for PHB crystallization to occur and less perfect crystals tended to develop at higher ϕ. The onset starting temperature of crystallization (T_0), crystallization peak temperature (T_p), the end crystallization temperature (T_e) and the crystallization enthalpy (ΔH_c) evolved were determined and the results given in Table II. It was clearly observed that as the ϕ increased both the T_0 and T_p shifted towards lower temperature, as expected. For example, T_0 and T_p decreased from 119 to 94°C and 113.3 to 76.4°C, respectively, when ϕ was increased from 2 to 50°C/min. A similar phenomenon was observed for a PHB/PLA/talc composite.[5,23] If the molten PHB was cooled down at a higher ϕ, there was insufficient time to overcome the nucleation energy barriers and more enthalpy was required for PHB chains to align orderly. Hence, the nucleation was being activated at lower temperature, which resulted in the delay of initiation of crystallization, lowering of T_0 and T_e values, and increasing ΔH_c (J/g) accordingly.[5] Whereas, upon slower cooling, the polymer chains have sufficient time to take on a more orderly configuration, hence the crystallization was initiated at an early stage so that higher T_0 values were observed. This provided practical guidance to the PHB products industrial melt processing. For example, in the injection molding processing, if the molder's temperature is set to be higher (slower crystallization rates), longer crystallization time would be required than samples are molded at lower temperature (faster crystallization rates). The properties of the final products would vary because coarser crystal structures with possible defects may form as compared with those (with finer crystal structures) being cooled at slower rates.

Nonisothermal Crystallization Kinetics Analysis by Different Models

Previous nonisothermal crystallization kinetic studies of PHB were focused on a relatively narrow cooling rate range or used limited models.[35] Therefore, this study used a wider range of cooling rates and developed models based on Liu and Mo's analysis and Jeziorny-modified-Avrami models to investigate PHB. In order to obtain more systematic kinetic information,

Table II. Values of the Heat Evolved During Nonisothermal Crystallization (ΔH_c, J/g), the T_0, T_c, T_p, and the Half-Time of the Crystallization ($t_{noniso\text{-}1/2}$) for PHB Determined from Figure 7(a), and Z_c Values Obtained by the Jeziorny-Modified-Avrami Analysis

$X_{t\text{-}noniso}$ (%)	$F(T)$	α	$\Delta E_{noniso\text{-}Kinsinger}$ (kJ/mol)	$\Delta E_{noniso\text{-}Friedman}$ (kJ/mol)
20	10.01	1.50	115.6	96.1
40	13.02	1.55		97.6
60	14.44	1.57		98.3
80	18.92	1.59		100.8

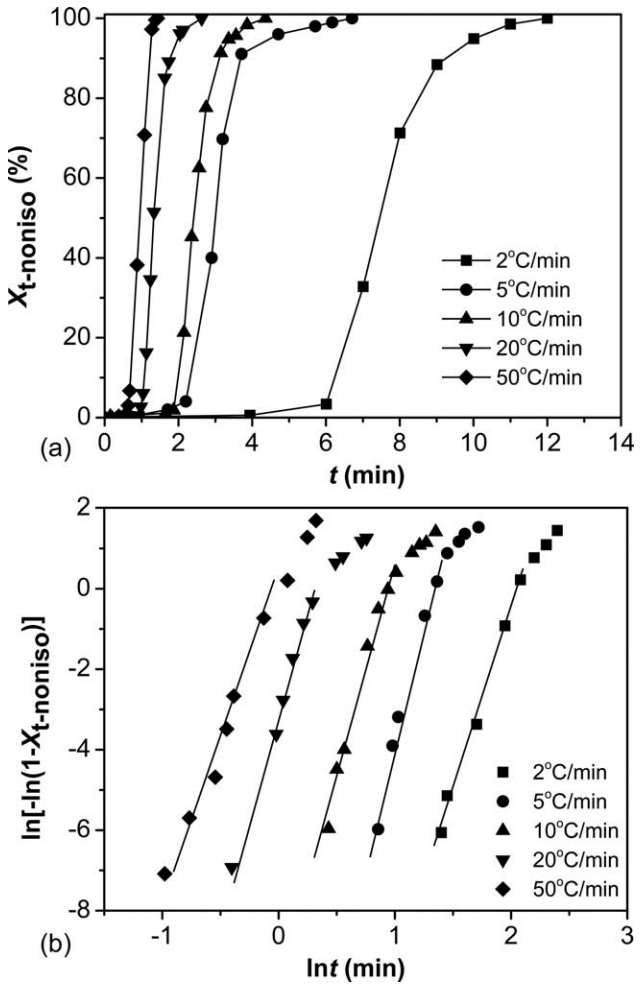

Figure 7. (a) Plot of relative crystallinity, $X_{t\text{-noniso}}$ (%), as function of time, t, and (b) plot of $\ln[-\ln(1 - X_{t\text{-iso}})]$ versus $\ln t$ of nonisothermal crystallization at different cooling rates (labeled in plot).

the raw data such as those shown in Figure 7 was presented as the relative crystallinity ($X_{t\text{-noniso}}$) as a function of temperature as follows:[5]

$$X_{t-\text{noniso}} = \int_{T_0}^{T} (dH_c/dT)dT \Big/ \int_{T_0}^{T_\infty} (dH_c/dT)dT \qquad (7)$$

where T_0 and T are the initial crystallization temperature and an arbitrary temperature, respectively. T_∞ was the end crystallization temperature and dH_c/dT was the heat flow rate. Once this relation was constructed the conversion from raw data into the $X_{t\text{-noniso}}$ as function of time, t, was obtained by transforming the temperature scale into a time scale according to:

$$t = (T_0 - T)/(\phi) \qquad (8)$$

where T is the temperature at time t, T_0 is the temperature at which crystallization begins ($t = 0$).

Figure 7(a) shows the plots of relative degree of crystallinity ($X_{t\text{-noniso}}$ %) as function of crystallization time at various ϕ. From this plot the half-time of crystallization, $t_{\text{noniso-1/2}}$, was obtained (Table II). It was clearly shown that by increasing ϕ, $t_{\text{noniso-1/2}}$ values were reduced. For example, at $\phi = 50$°C/min, $t_{\text{noniso-1/2}}$ was only 1 min, suggesting that such a high ϕ can encourage the crystallization to occur faster. This implies the use of "nucleation agent" could be avoided if PHB is processed under higher cooling rates, because the crystals formed at earlier crystallization stage could play a role of "crystal seeding". This can be applied to explain the flash $t_{\text{cry-1/2}}$ at $T_{\text{iso}} = 80$ and 90°C.

As mentioned above, the Avrami equation was applied to explain the isothermally induced crystallization, whereas during the nonisothermal crystallization process the parameters k and n will depend upon both the rates of nucleation and crystal growth process.[5,36] This was further confirmed by the straight line obtained from the plot of $\ln[-\ln(1\text{-}X_{t\text{-noniso}})]$ versus $\ln t$ at the early stage of crystallization followed by a large deviation [Figure 7(b)]. Jeziorny modified this model to describe the nonisothermal crystallization process with changing ϕ. Most recently Deshmukh and his coworkers successfully used this model to investigate the nonisothermal crystallization kinetics of PBT (based composites).[15] Hence, semicrystalline PHB was expected to be explained by Jeziorny-modified-Avrami model. To consider the effect of ϕ on the rate constant, k was corrected by assuming a constant, Z_c, and then the modified form of the parameter to characterize the kinetics of nonisothermal crystallization was established:[15]

$$\ln Z_c = \ln k/(\phi) \qquad (9)$$

where Z_c is the Jeziorny constant.

From Table II, Z_c values reflecting the crystallization rate were increased with increasing ϕ. The crystallization rate depends on the rates of nucleation and nuclei growth.[5] Higher ϕ induces a higher extent of undercooling, resulting in an increase of nucleation density, and hence the crystallization rate will be increased accordingly. Thus, the Avrami model did not describe the kinetics of nonisothermal crystallization observed. However, the Jeziorny-modified-Avrami theory was able to describe successfully the kinetic behavior of nonisothermal crystallization of PHB.

By simple modification, Ozawa extended the Avrami equation to describe the nonisothermal crystallization kinetics.[40] Based on his assumption, the nonisothermal crystallization process was to be comprised of infinitesimally small isothermal crystallization steps at a conditional temperature (T) and expressed as:

$$1 - X_{t-\text{noniso}|T} = \exp[-K(T)/(\phi)^m] \qquad (10)$$

and this equation can be rearranged to be in double-logarithmic form:

$$\ln[-\ln(1 - X_{t-\text{noniso}|T})] = \ln[K(T)] - m\ln(\phi) \qquad (11)$$

where $K(T)$ is the cooling function and m is the Ozawa exponent depending on the crystal growth. If the Ozawa model is valid, the explanation of the nonisothermal crystallization of PHB in this study would give a straight line for the plot of $\ln[-\ln(1 - X_{t\text{-noniso}|T})]$ versus $\ln(\phi)$, from which the $K(T)$ and m can be obtained. The Ozawa plot based on eq. (11) at specific temperatures of PHB is shown in Figure 8. The Ozawa plots clearly shows deviation from linearity and m varies at various ϕ, suggesting the Ozawa analysis was not successful

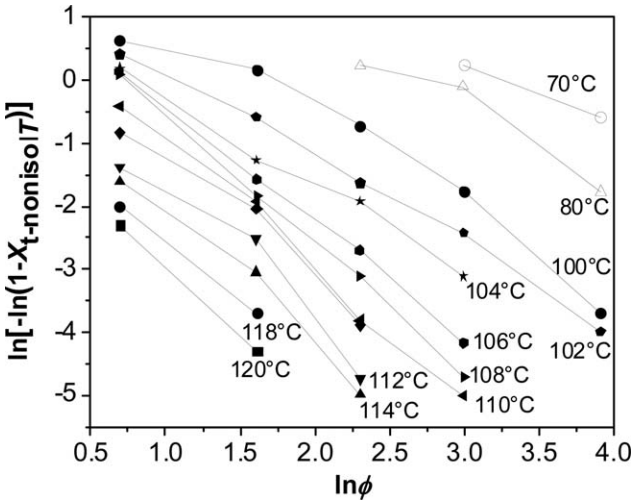

Figure 8. Ozawa plots of $\ln[-\ln(1-X_{\text{t-noniso}|T})]$ versus $\ln\phi$ for nonisothermal crystallization of PHB.

in explaining the nonisothermal crystallization kinetics of PHB. This may be ascribed to either a change in crystallization mechanism or secondary crystallization which has been ignored in Ozawa's model.[15]

To further explain the nonisothermal crystallization kinetics of PHB, a new model was proposed by Liu and Mo which combined the Avrami and Ozawa's equations as follows:[14]

$$\ln\phi = \ln F(T) - \alpha \ln t \tag{12}$$

where $F(T) = [K(T)/k)^{1/m}]$ is the ϕ that needs to reach a defined degree of crystallinity at a unit of crystallization time, α is the ratio between the Avrami exponent, n, and the Ozawa exponent, m, namely n/m. By plotting $\ln\phi$ versus $\ln t$ at selected relative degree of crystallinity ($X_{\text{t-noniso}}$), the $F(T)$ and α can be obtained from the intercept and slope of the fitted straight line, respectively. These values are listed in Table III. It can be seen that PHB exhibits a linear relationship between $\ln\phi$ and $\ln t$ at given $X_{\text{t-noniso}}$ values of 20, 40, 60, and 80%, and α values varies from 1.50 to 1.59. The variation in α was small, indicating that the Liu and Mo's model was appropriate to describe the nonisothermal crystallization kinetics of PHB. The value of $F(T)$ increased with an increase of $X_{\text{t-noniso}}$, suggesting that at a unit crystallization time a higher degree of crystallinity will be achieved with a higher ϕ. Similar findings were reported for polylactic acid/PHB blends,[5] polybutyleneterphalate,[15] and polypropylene.[36] This result is consistent with the Jeziorny-modified-Avrami analysis. It can be concluded that the Liu and Mo's analysis is a suitable model to explain the nonisothermal crystallization behavior of PHB in this study. As a result, the nonisothermal crystallization kinetics studies implied the degree of crystallinity of PHB final products could be monitored by the nonisothermal conditions (cooling rates). This also explained why nucleation agents are commonly added to facilitate the crystallization process of PHB based copolymers, PHBV.

Activation Energy in Nonisothermal Crystallization Process

To evaluate the activation energy involved during the nonisothermal crystallization process with different ϕ, the Kissinger's method was primarily used:[5]

$$\mathrm{d}\left[\ln\left(\phi/T_p^2\right)\right]/\mathrm{d}\left(1/T_p\right) = \text{Constant} - \Delta E_{\text{noniso-Kinsinger}}/RT_p \tag{13}$$

where R is the universal gas constant and $\Delta E_{\text{noniso-Kinsinger}}$ is the activation energy of crystallization. From the plot of $\ln(\phi/T_p^2)$ versus $1/T_p$ [Figure 9(a)], the $\Delta E_{\text{noniso-Kinsinger}}$ was determined from slope of the fitted straight line as 115.6 kJ/mol (Table III). This value was slightly higher than the result of 92.6 kJ/mol reported by An *et al.*,[35] which might be caused by differences of M_w and molecular weight distribution.

Recently, the differential isoconversional method of Friedman and the advanced integral isoconversional method of Vyazovkin were found to be more appropriate than the Kissinger's method.[37] In this study, the method of Friedman was used to validate the activation energy of the nonisothermal crystallization process.

The Friedman equation is expressed as follows:[37]

$$\ln[dX_{\text{t-noniso}}/dt]_{X,\,i} = \text{constant} - \Delta E_{\text{noniso-Friedman}}/RT_{X,\,i}$$

where $dX_{\text{t-noniso}}/dt$ is the instantaneous crystallization rate as a function of time at a given conversion $X_{\text{t-noniso}}$. The $dX_{\text{t-noniso}}/dt$ was obtained by integrating the $X_{\text{t-noniso}}$ with respect to the time that needed to reach to a relative degree of crytallinity ($X_{\text{t-noniso}}$). By selecting an appropriate $X_{\text{t-noniso}}$ (i.e., from 2 to 98%) the values of $dX_{\text{t-noniso}}/dt$ at a specific $X_{\text{t-noniso}}$ are correlated to the corresponding crystallization temperature at this $X_{\text{t-noniso}}$, that is, $T_{X,i}$.

The Friedman plot of $\ln[dX_{\text{t-noniso}}/dt]$ versus $1/T_{X,i}$ for PHB at different relative crystallinities ($X_{\text{t-noniso}} = 20$, 40, 60, and 80%) is shown in Figure 9(b). The $\Delta E_{\text{noniso-Friedman}}$ values determined from the straight lines ($R^2 = 0.99$) at selected $X_{\text{t-noniso}}$ are shown in Table III. It can be seen that $\Delta E_{\text{noniso-Friedman}}$ ranges from 96.1 to 100.8 kJ/mol. This is slightly lower than the activation energy obtained from Kinsinger's model.

Crystallization activation energy was a good indicator for the crystallization ability of polymers, hence the higher ΔE_{noniso} values reveal that it was more difficult for PHB to transport polymer chains segments to grow on the surfaces of previously formed crystals. However, apart from the higher activation energy obtained, the other kinetics parameters such as $t_{\text{noniso-1/2}}$ and Z_c clearly showed that the higher ϕ could enhance the PHB crystallization rate. By comparing the activation energy between different polymers (e.g., PHB and PHBV), the flexibility of these materials can be predicted. If the work of chain-folding is less, then the material would be more suitable as packaging because of higher flexibility.

Effect of Cooling Rate on the Melting Behavior

Semicrystalline polymers are usually processed nonisothermally from melt; hence it was important to investigate the subsequent melting behavior of PHB after it had finished nonisothermal crystallization at different ϕ. The DSC curves of the melting behavior of PHB are shown in Figure 10. After the nonisothermal crystallization process from melt at different ϕ, ranging from 2 to 50°C/min, the conventional DSC heating scans were recorded at Φ of 10°C/min [Figure 10(a)]. If the ϕ was set at

Table III. Nonisothermal Crystallization Kinetic Parameters at Different Degree of Relative Crystallinity ($X_{t\text{-noniso}}$) Determined from Liu and Mo's Analysis and Activation Energy Values Based on Kinsinger's ($E_{noniso\text{-}Kinsinger}$) and Friedman ($E_{noniso\text{-}Friedman}$) Models

Cooling rate (°C/min)	T_0 (°C)	T_p (°C)	T_e (°C)	$t_{noniso\text{-}1/2}$ (min)	ΔH_c (J/g)	Z_c
2	119.1	113.3	107.2	7.4	86.4	0.7424
5	114.3	106.8	99.4	3.0	84.2	0.7803
10	109.3	100.4	92.9	2.5	77.9	0.7943
20	103.1	92.2	78.3	1.4	72.4	0.8122
50	94.1	76.4	52.7	1.0	59.9	0.8831

2°C/min, only one broad melting peak was observed. Whereas by increasing the ϕ to 5°C/min or higher, two endothermic peaks (labeled as T_{m1} and T_{m2} in the order of low to high temperature) started showing up and the higher endotherm (T_{m2}) was more clearly to be seen at higher ϕ (10 to 50°C/min). The T_{m1} values shifted from 165.0 to 161.5°C when ϕ was increased from 5 to 50°C/min, while T_{m2} was not changed and located at 170°C that is close to the T_{melt} obtained by TMA. The similar multiple melting behavior was also observed in other nonisothermally crystallized semicrystalline polymers from melt, such as PBSU and PES which was regarded as the evidence for the melting-recrystallization mechanism.[16] The effect of ϕ on the degree of crystallinity ($X_{noniso\text{-}melt}$) of PHB was determined according to eq. (6) from the melting enthalpies of the endothermic curves [Figure 10(a)]. The $X_{noniso\text{-}melt}$ values were 54, 56, 58, 60, and 63%, respectively, when $\phi = 2$, 5, 10, 20, and 50°C/min. This confirmed that the higher ϕ results in more crystalline PHB, which agrees with the kinetic study by Liu and Mo's model.

Although the MRR was assumed to occur during DSC heating scans, the exothermic peak was hard to detect by conventional DSC due to superposition of the recrystallization and the melting endotherms.[21] Therefore, TMDSC was used to prove the melting-recrystallization behavior during the heating scan; meantime, the T_g (~5°C) was obtained from the heating scans. Figure 10(b) shows an example of TMDSC melting scans of PHB following the nonisothermally crystallization at $\phi = 10$°C/min. The total heat flow (T) curve was separated into the nonreversing (Non-Rev) and reversing (Rev) curves. Unlike the conventional DSC traces shown in Figure 10(a) where no recrystallization exotherm was seen at a heating rate of 10°C/min, one crystallization exotherm [Figure 10(b), labeled as Exo] was observed by TMDSC between the two endothermic peaks in the Rev curve because the time was long enough for crystallites involved in low melting endotherm with low thermal stability to experience the melting and recrystallization at a heating rate of 2°C/min. The higher endotherm was the dominant peak which was in accordance with conventional DSC and similar finding was observed in literature.[29,40] All these results confirmed the assumption that the multiple melting behavior observed in the nonisothermally crystallized PHB was ascribed to the MRR mechanism of crystallites of the low melting endotherm with low thermal stability. This finding was in good agreement with studies on different polymers.[16]

Effects of Heating Rate on the Melting Behavior of PHB Studied by DSC

From the literature, the MRR model is often used to explain the multiple melting behavior depending on the heating scan rates.[20] In this study, heating scans as function of different Φ were recorded after PHB samples were quenched to −50°C, and then heated to 200°C using conventional DSC [Figure 11(a)]. It can be seen that two melting endotherms appear when Φ was

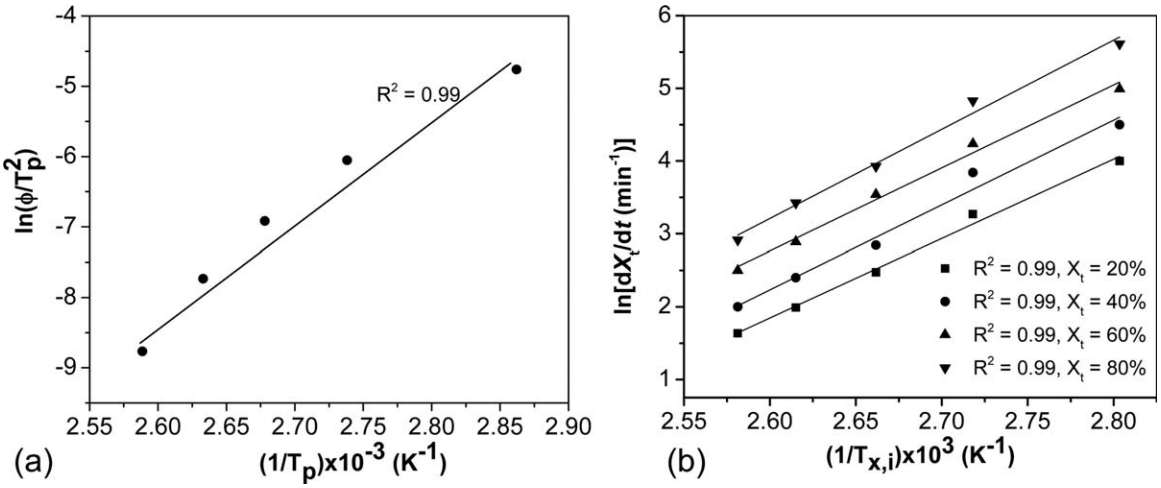

Figure 9. (a) Kissinger's ($\ln(\phi/T_p^2)$ vs. $1/T_p$) and (b) Friedman ($\ln(dX_{noniso}/dt)$ versus $1/T_{x,i}$ at different degree of crystallinity) plot for nonisothermal crystallization of PHB.

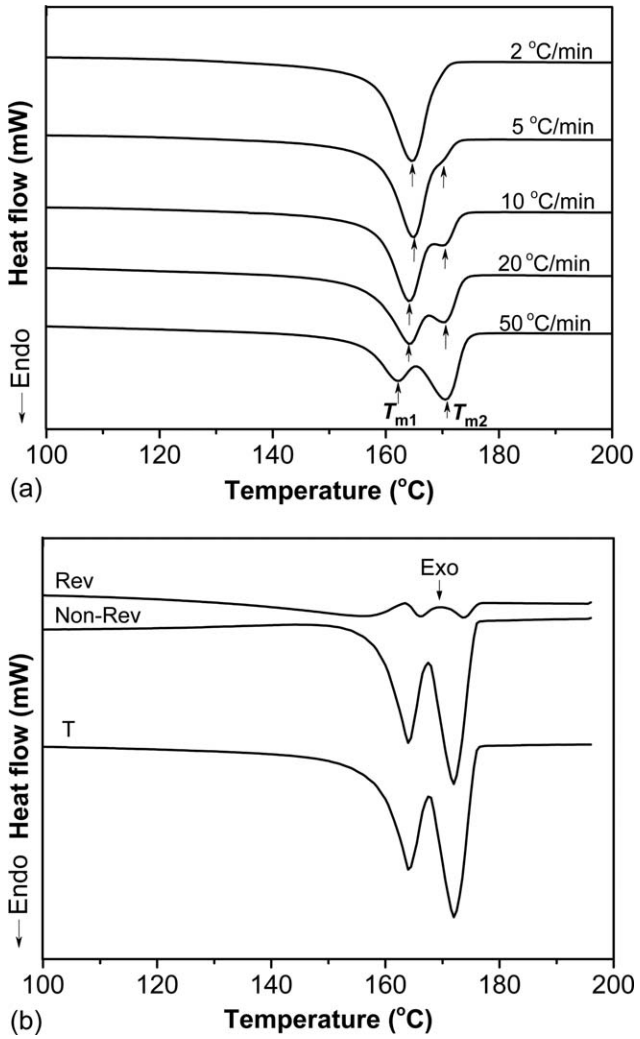

Figure 10. (a) Conventional DSC and (b) TMDSC curves of the melting behavior of PHB after nonisothermal crystallization.

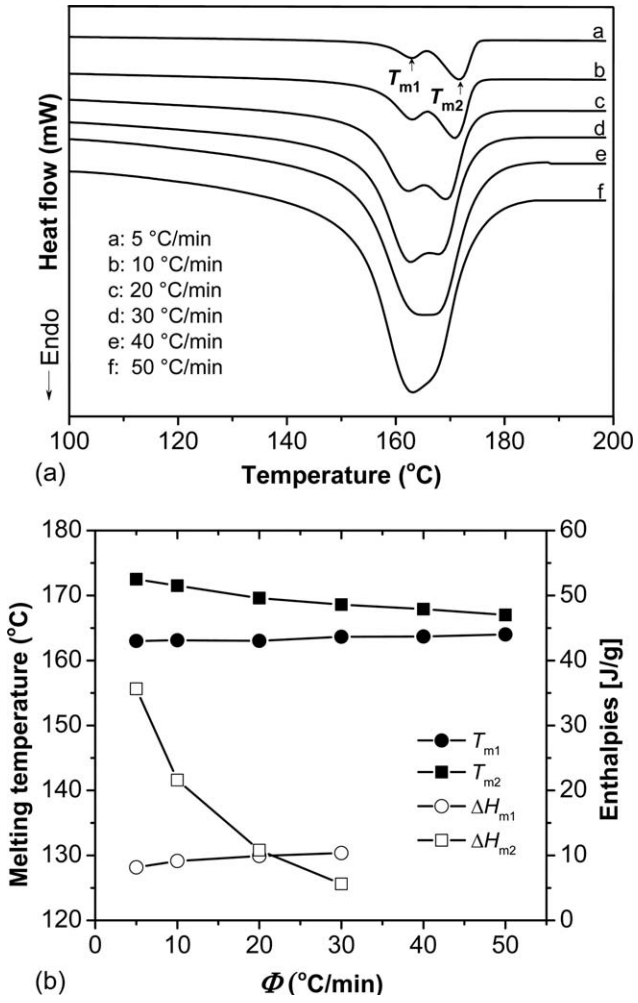

Figure 11. (a) DSC heating scans and (b) melting temperatures (T_{m1} and T_{m2}) and their corresponding enthalpies (ΔH_{m1} and ΔH_{m2}) for PHB performed at different heating rates (Φ).

<30°C/min, and when the Φ was increased > 40°C/min, the two melting endotherms merged into one broad peak. The peak values of these two endotherms (labeled as T_{m1} and T_{m2} in the order of temperature from low to high) and their corresponding enthalpies associated were determined and plotted in Figure 11(b). With an increase in Φ the T_{m1} shifted slightly from 164 to 164.5°C, while T_{m2} was decreased slightly from 172 to 168°C, and the magnitude of T_{m1} was increased as indicated by the increase of ΔH_{m1}. Whereas, ΔH_{m2} was shown to decrease significantly as Φ increased from 5 to 30°C. At higher Φ, recrystallization was limited by less time available to align chains and form new crystals, consequently the amount and perfection of the reorganized crystals will be reduced, resulting in a slight decrease of T_{m2}.[20] This further confirms the assumption that the MRR model can explain the multiple/double melting behavior of PHB. In other words, the slightly lowered T_{m1} (higher cooling rates) and T_{m2} (higher heating rates) suggest a decrease in processing temperature can be achieved. This means thermal degradation during melting processing can be avoided to some extent.

CONCLUSIONS

The annealing-temperature-dependent multiple melting and recrystallization behavior of PHB was studied by conventional DSC and TMDSC. It was found that PHB showed multiple melting peaks, annealing peak (T_{ap}) and two melting peaks (T_{m1} and T_{m2}), after being annealed at different temperatures (T_a) and same time. The T_{m1} was not influenced by T_a, but the T_{m2} was associated with T_a. The degree of crystallinity (χ_c%) was shown to depend on annealing temperature. When T_a was <100°C and >120°C the χ_c% decreased with increasing T_a, but only showed a slight change when 100°C < T_a <120°C. It could be expected that lower annealing temperature will result in higher crystallinity end products and more amorphous PHB will be obtained if higher annealing temperature will be applied in the PHB manufacturing procedure. The higher isothermal annealing temperature will inhibit the recrystallization behavior, resulting in a single melting endotherm. It was concluded that T_a = 100°C was a suitable isothermal T_a for PHB. Wider isothermal temperature range (T_{iso} = 80 to 140°C) was selected to investigate the isothermal crystallization kinetics of PHB.

Nonisothermal crystallization studies showed dual melting peaks at high cooling rates (ϕ) ~10°C/min. The Jeziorny-modified-Avrami method and Liu-Mo's analysis were successful in describing the nonisothermal crystallization kinetics of PHB, while the Ozawa model was not. The multiple melting behaviors were also heating-rate-dependent and at a high heating rate (Φ, 40°C/min) the multiple melting peaks merged into one. The higher endothermic peak (T_{m2}) was not affected by ϕ and T_{m2} decreased slightly with increasing Φ. T_{m1} was considered to be related to the original crystals before analysis while the T_{m2} was ascribed to the recrystallization of crystals with lower thermal stability showing an endotherm at T_{m1}. In brief, the higher melting peak induced by either isothermally or nonisothermally was mainly ascribed to melting-recrystallization-remelting mechanism (MRR) during DSC heating scans, and the TMDSC technique allows the observation of the recrystallization present in the heating process more clearly. The activation energies were estimated in isothermal and nonisothermal crystallization process to be 102 and 116 kJ/mol, respectively. This study has provided insight into the thermal history and property (especially the crystallinity involved in the isothermal/nonisothermal process) relationship, giving theoretical guidance to the PHB industrial processing (e.g., injection molding and extrusion) and product applications.

ACKNOWLEDGMENTS

We would like to acknowledge the financial support from a USDA-Forest Products Laboratory grant 08-JV-111111 and USDA-CSREES grant 2007-34158-17640 for supporting the DSC instrument.

REFERENCES

1. Madison, L.; Huisman, G. W. *Microbiol. Mol. Biol. Rev.* **1999**, *63*, 21.
2. Khanna, S.; Srivastava, A. K. *Process Biochem.* **2005**, *40*, 607.
3. Wei, L.; McDonald, A. G. *J. Appl. Polym. Sci.* **2015**, *132*, Doi: 10.1002/app.41724.
4. Wei, L.; Guho, N. M.; Coats, E. R.; McDonald, A. G. *J. Appl. Polym. Sci.* **2014**, *131*, DOI: 10.1002/app.40333.
5. Tri, P. N.; Domenek, S.; Guinault, A.; Sollogoub, C. *J. Appl. Polym. Sci.* **2013**, *129*, 3355.
6. Wei, L.; McDonald, A. G.; Stark, N. M. *Biomacromolecules* **2015**, *16*, 1040.
7. Chen, C.; Peng, S.; Fei, B.; Zhuang, Y.; Dong, L.; Feng, Z.; Chen, S.; Xia, H. *J. Appl. Polym. Sci.* **2003**, *88*, 659.
8. Roa, J. P.; Patrício, P. S. D. O.; Oréfice, R. L.; Lago, R. M. *J. Appl. Polym. Sci.* **2013**, *128*, 3019.
9. Wang, L.; Zhu, W.; Wang, X.; Chen, X.; Chen, G.-Q.; Xu, K. *J. Appl. Polym. Sci.* **2008**, *107*, 166.
10. Wang, T.; Cheng, G.; Ma, S.; Cai, Z.; Zhang, L. *J. Appl. Polym. Sci.* **2003**, *89*, 2116.
11. Long, Y.; Shanks, R. A.; Stachurski, Z. H. *Prog. Polym. Sci.* **1995**, *20*, 651.
12. An, Y.; Dong, L.; Li, L.; Mo, Z.; Feng, Z. *Eur. Polym. J.* **1999**, *35*, 365.
13. Wang, Y. D.; Yamamoto, T.; Cakmak, M. *J. Appl. Polym. Sci.* **1996**, *61*, 1957.
14. Liu, T.; Mo, Z.; Wang, S.; Zhang, H. *Polym. Eng. Sci.* **1997**, *37*, 568.
15. Deshmukh, G. S.; Peshwe, D. R.; Pathak, S. U.; Ekhe, J. D. *Thermochim. Acta* **2014**, *581*, 41.
16. Qiu, Z.; Komura, M.; Ikehara, T.; Nishi, T. *Polymer* **2003**, *44*, 7781.
17. Gunaratne, L. M. W. K.; Shanks, R. A. *J. Polym. Sci. Part B: Polym. Phys.* **2006**, *44*, 70.
18. Rizk, S.; Connelly, D. W.; Bernasconi, M.; Carter, A. J.; Martin, D. P.; Williams, S. F. U.S. Patent 20130309166 A1, USA. **2013**.
19. Montserrat, S.; Roman, F.; Colomer, P. *J. Therm. Anal. Calorim.* **2003**, *72*, 657.
20. Liu, T.; Petermann, J. *Polymer* **2001**, *42*, 6453.
21. Qiu, Z.; Ikehara, T.; Nishi, T. *Polymer* **2003**, *44*, 3095.
22. Hu, S.; McDonald, A. G.; Coats, E. R. *J. Appl. Polym. Sci.* **2013**, *129*, 1314.
23. He, J.-D.; Cheung, M. K.; Yu, P. H.; Chen, G.-Q. *J. Appl. Polym. Sci.* **2001**, *82*, 90.
24. Gunaratne, L. M. W. K.; Shanks, R. A. *J. Therm. Anal. Calorim.* **2006**, *83*, 313.
25. Gunaratne, L. M. W. K.; Shanks, R. A. *Eur. Polym. J.* **2005**, *41*, 2980.
26. Hu, Y.; Zhang, J.; Sato, H.; Futami, Y.; Noda, I.; Ozaki, Y. *Macromolecules* **2006**, *39*, 3841.
27. Kong, Y.; Hay, J. N. *Polymer* **2003**, *44*, 623.
28. Minakov, A. A.; Mordvintsev, D. A.; Schick, C. *Polymer* **2004**, *45*, 3755.
29. Puente, J. A. S.; Esposito, A.; Chivrac, F.; Dargent, E. *J. Appl. Polym. Sci.* **2013**, *128*, 2586.
30. Kampert, W. G.; Sauer, B. B. *Polym. Eng. Sci.* **2001**, *41*, 1714.
31. Sauer, B. B.; Kampert, W. G.; Blanchard, E. N.; Threefoot, S. A.; Hsiao, B. S. *Polymer* **2000**, *41*, 1099.
32. Hoffman, J. D. *Polymer* **1982**, *23*, 656.
33. Pogodina, N. V.; Winter, H. H. *Macromolecules* **1998**, *31*, 8164.
34. Wei, L.; McDonald, A. G.; Freitag, C.; Morrell, J. *J. Polym. Degrad. Stab.* **2013**, *98*, 1348.
35. An, Y.; Dong, L.; Mo, Z.; Liu, T.; Feng, Z. *J. Polym. Sci., Part B: Polym. Phys.* **1998**, *36*, 1305.
36. Yuan, Q.; Awate, S.; Misra, R. D. K. *Eur. Polym. J.* **2006**, *42*, 1994.
37. Friedman, H. *J. Polym. Sci. Part C: Polym. Symp.* **1964**, *6*, 183.